

Ultrathin Printable Graphene Supercapacitors with AC Line-Filtering Performance

Zhong-Shuai Wu, Zhaoyang Liu, Khaled Parvez, Xinliang Feng,* and Klaus Müllen*

Printed electronics is an emerging technology representing greatly integrated functionality of thinness, flexibility, scalability, and light weight, and has enormous potential applications of such as printable transistors, photovoltaic cells, flexible displays, sensors, radio frequency identification, and organic light-emitting diodes, which have ultimately stimulated the rapid development of new-concept, miniaturized printable energy-storage systems that can be compatible with them.^[1–6] In this respect, printable supercapacitors, commonly fabricated using printed films on plastic or paper substrates, have been widely acknowledged as an ideal power source for printed electronics because they can incorporate multiple functions in a single device.^[7–13] In the last few years, the scalability, flexibility, and performance of printable supercapacitors have been advanced through the fabrication of various thin films: i) with nanostructured active materials, e.g., carbon nanotubes,^[7] activated carbon,^[14] cobalt hydroxide,^[15] carbon nanotubes/RuO₂,^[16] and graphene/polyaniline;^[17] ii) on different flexible substrates with a thickness of >200 μm,^[7,13–18] including paperboard,^[13] poly(ethylene terephthalate) (PET),^[7,16,18] polyester film,^[15] cloth fabrics,^[16] carbon fabrics;^[17] and iii) utilizing scalable manufacturing processes, e.g., inkjet printing,^[16,19] spray-coating,^[7,18] screen-printing,^[17] and roll-to-roll processing.^[20] Nevertheless, the overall scalability, flexibility, and electrochemical performance of these printable supercapacitors, especially, related to the entire device thickness (>400 μm, with two substrates,^[7,16,18] rate performance ($\leq 0.5 \text{ V s}^{-1}$),^[7,17] and frequency response (a typical resistor-capacitor (RC) time constant of 1 s^[21]) are far from satisfactory.

To implement high-frequency operation in most line-powered electronics, alternating current (AC) line-filtering is a key parameter that can attenuate the leftover AC ripples on direct current voltage busses.^[21–23] Because the large-volume and heavy component of popular aluminum electrolytic capacitors (AECs) mostly hinder small-size filtering applications, particularly in some portable electronic circuits, the development of more compact supercapacitors capable of replacing AECs for filtering voltage ripples is becoming one of the major tasks for future electronics.^[21] Typically, porous carbon supercapacitors

perform poorly at 120 Hz, with a typical impedance phase angle near 0° and a RC time constant of 1 s, both of which are far from the competitive requirements for filtering (close to a –90° value and a RC time constant period of ca. 8.3 ms) because of the complex porous structure of the carbon electrodes.^[23] Recently, remarkable achievements were made by Miller et al.^[21] and Sheng et al.,^[22] who demonstrated that supercapacitors utilizing vertically oriented graphene sheets grown on nickel substrates by chemical vapor deposition (CVD)^[21] and electrochemically reduced graphene oxide (ErGO) films on Au foil^[22] could efficiently filter a 120 Hz ripple. Unfortunately, the fabrication of these graphene electrodes grown/deposited on metal (Ni, Au) current collectors requires a high-cost and complicated manufacturing process.

In this work, we demonstrate the fabrication of ultrathin printable supercapacitors (UPSCs) with AC line-filtering performance based on graphene-conducting polymer (EG/PH1000) hybrid films. The conductive hybrid ink of electrochemically exfoliated graphene (EG) and poly(3,4-ethylenedioxythiophene):poly(styrenesulfonate) (PEDOT:PSS) (Clevios PH1000) was spray coated on a gold-deposited 2.5-μm-thick PET substrate with a tunable thickness ranging from nanometers to micrometers. Thus, the UPSCs were constructed with two EG/PH1000 hybrid films sandwiching a thin polymer gel electrolyte of poly(vinyl alcohol)/H₂SO₄ (PVA/H₂SO₄) and exhibited an unprecedented volumetric capacitance of 348 F cm⁻³ and excellent cycling stability with no capacitance loss after 50 000 cycles. Such UPSCs could be operated at an ultrahigh rate of up to 2000 V s⁻¹. More importantly, our devices delivered an AC line-filtering performance with an extremely short RC time constant of <0.5 ms.

To fabricate the UPSCs (See **Figure 1**), we first selected a 30 nm Au-coated PET substrate (2.5 μm thick, Figure S1, Supporting Information) as the thin-film support. The thin Au layer can function as a current collector, which is helpful to effectively collect/transport charge carriers (e.g., electrons) from/to the active materials during the charge and discharge processes.^[24,25] Afterward, a highly stable ink (1 mg mL⁻¹ of EG, 20% PH1000), composed of high-quality EG^[26,27] (Figure S2, Supporting Information) and PH1000 polymer in *N,N'*-dimethylformamide, was readily prepared by sonication for 1 h (Figure 1a,b and Figure S3, Supporting Information). Then, the EG/PH1000 films were manufactured by coating the solution-processable ink onto an ultrathin PET substrate using the spray painting technique (Figure 1c).^[28] To assist the formation of the uniform film (Figure 1d) and the subsequent assembly of the ultrathin device (Figure 1e–h), a stable poly(dimethylsiloxane) (PDMS) substrate was attached underneath the PET substrate before coating (Figure 1e,f). Subsequently, a polymer gel electrolyte of PVA/H₂SO₄ possessing excellent compatibility with the flexible PET/PDMS substrate was utilized as both the separator and the solid electrolyte, sandwiched

Dr. Z.-S. Wu, Z. Liu, Dr. K. Parvez, Prof. K. Müllen
Max-Planck-Institut für Polymerforschung
Ackermannweg 10, 55128 Mainz, Germany
E-mail: muellen@mpip-mainz.mpg.de

Prof. X. L. Feng
Department of Chemistry and Food Chemistry and
Center for Advancing Electronics Dresden (CFAED)
Technische Universität Dresden
01062 Dresden, Germany
E-mail: xinliang.feng@tu-dresden.de



DOI: 10.1002/adma.201501208

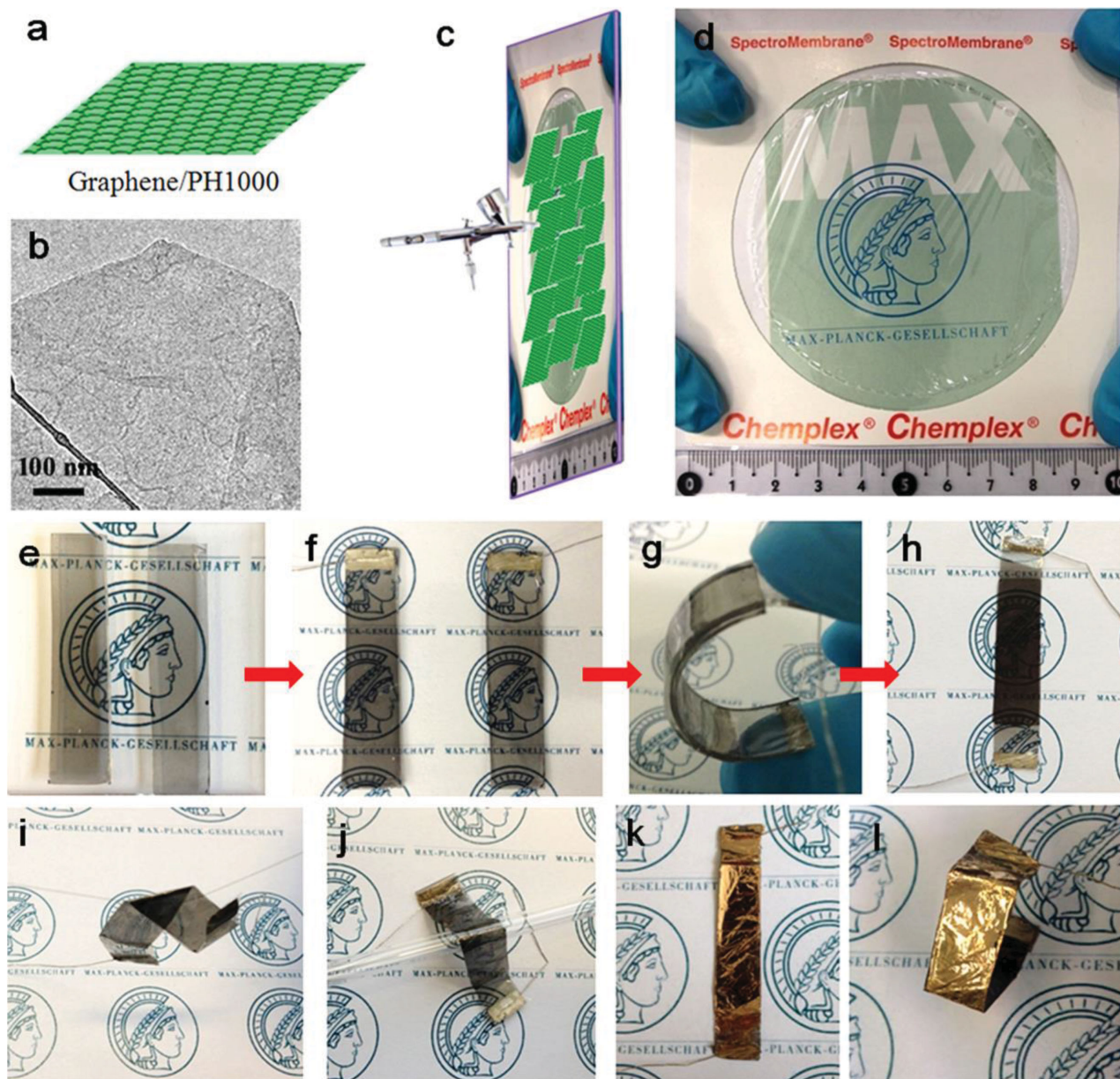


Figure 1. Schematic illustration of UPSCs. a) Schematic description of 2D EG/PH1000 nanosheets. b) TEM image of the PH1000 adsorbed EG nanosheets. c) Fabrication scheme of EG/PH1000 film on 2.5- μm -thick PET substrate with an air brush pistol. d) Optical image of the EG/PH1000 film on a 2.5- μm -thick PET substrate with a thin-film diameter of 76 mm. e–h) Optical images showing the fabrication of UPSCs, including: e) spray coating of EG/PH1000 film on 2.5- μm -thick PET/PDMS substrates, with lengths of 4.5 cm and widths of 1 cm; f) coating of gel electrolyte on the surface of film electrodes and connection of the Pt wire on the film by silver paste glue; g) assembly of UPSCs sandwiched between two gel-electrolyte/film electrodes on PET/PDMS substrates; h) all-solid-state UPSCs on 2.5- μm -thick PET substrates (after peeling off the PDMS substrates). i–l) UPSCs with excellent flexibility, e.g., naturally bending state when: i) hung on a hair and j) placed on a NMR glass tube. k, l) A UPSC based on EG/PH1000 film on Au-coated PET substrates (with the same procedure as (e–g)), showing: k) flat and l) folded bending states.

between two film electrodes (Figure 1f,g).^[29,30] Finally, a UPSC was constructed based on EG/PH1000 films on ultrathin PET substrates after peeling off the PDMS substrates (Figure 1h–l, see details in the Experimental Section).

The surface topography of the EG/PH1000 hybrid film was examined by scanning electron microscopy (SEM) and atomic force microscopy (AFM) (Figure 2 and Figure S4, Supporting Information). The low-magnification SEM images reveal

the formation of large-area, uniform and continuous films (Figure 2a). The high-magnification SEM images reveal the presence of small segments of the PH1000 polymer covered on the flat EG sheets (Figure 2b and Figure S4, Supporting Information). The AFM images support the compact coating of graphene and PH1000 on the films with a low average surface roughness, root-mean-square (RMS) = 3.85 nm (Figure 2c,d). In addition, the obtained EG/PH1000 films exhibited a high

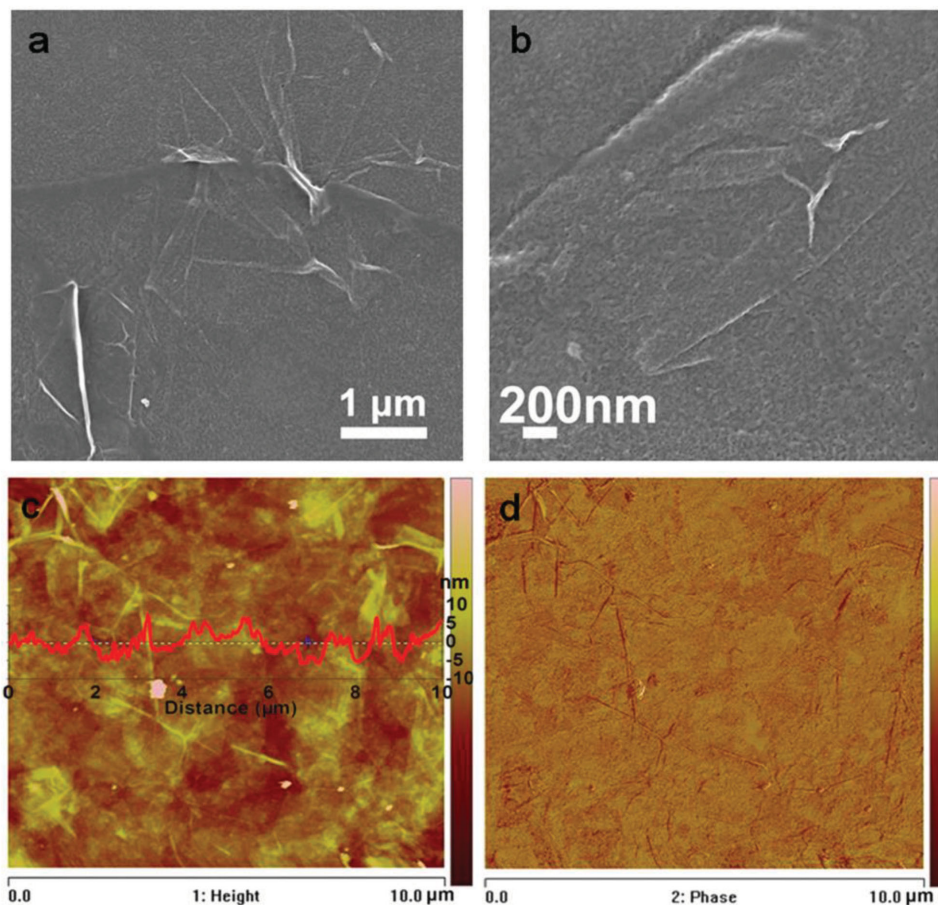


Figure 2. Morphology characterization of the spray-coated EG/PH1000 hybrid films. a) Low- and b) high-magnification SEM images of as-fabricated EG/PH1000 film (with 1 mL ink). c) AFM height image (the inset shows the height profile showing the low average surface roughness of the film with a RMS of 3.85 nm) and d) AFM phase image of the EG/PH1000 film.

electrical conductivity of about 1000 S cm^{-1} , measured by a standard four-point probe system.^[28]

The electrochemical properties of the as-fabricated UPSCs were first inspected from 1 to 2000 V s^{-1} using cyclic voltammetry (CV) (Figure 3). For the 25-nm-thick EG/PH1000 film-based UPSCs (denoted as UPSCs-25), a nearly rectangular CV shape was observed with a typical electrical double-layer capacitive behavior at scan rates from 1 to 1000 V s^{-1} (Figure 3a–d).^[29,31] A gradual increase of the discharge current of the CV curves was observed with increased scan rate (Figure 3a–e). Notably, this ultrathin device possessed ultrafast charging and discharging capability; for instance, a linear dependence of the logarithmic discharge current versus the scan rate was identified even up to 2000 V s^{-1} (Figure 3e,f). It should be emphasized that the scan rate of 2000 V s^{-1} is the highest value for electric double-layer capacitors (EDLCs) reported to date.^[32–34] Our set-up outperformed any high-power supercapacitor devices, e.g., onion-like carbon (200 V s^{-1}),^[35] ErGO (400 V s^{-1})^[22] and methane plasma rGO film (1000 V s^{-1}).^[33]

The areal capacitance and volumetric capacitance of UPSCs-25 as a function of scan rate are shown in Figure 4a. Remarkably, the device exhibited a maximum areal capacitance of 0.87 mF cm^{-2} (Figure 4a), which is superior to the values of reported graphene

thin-film supercapacitors, e.g., ErGO (0.49 mF cm^{-2}),^[22] methane plasma rGO film ($0.32\text{--}0.46 \text{ mF cm}^{-2}$),^[33,34] and laser-written GO film (0.51 mF cm^{-2}).^[36] Furthermore, the device can deliver an excellent volumetric capacitance of 348 F cm^{-3} (Figure 4a), which is much higher than the values of the state-of-the-art supercapacitors based on different graphene materials, e.g., liquid-electrolyte-mediated graphene film (261 F cm^{-3}),^[37] holey graphene framework (212 F cm^{-3}),^[38] aligned nanoporous microwave exfoliated GO film (177 F cm^{-3}),^[39] activated graphene (60 F cm^{-3}),^[40] laser-written GO film (3.1 F cm^{-3}),^[36] and laser-scribed graphene film (19 F cm^{-3}).^[41,42] Impressively, even at the ultrahigh rate of 2000 V s^{-1} , our supercapacitors can still achieve significant charge storage values of $43 \mu\text{F cm}^{-2}$ and 17.5 F cm^{-3} within an extremely short charging time of $<1 \text{ ms}$ (Figures 3e and 4a), suggestive of ultrahigh instantaneous power capability. The ultrahigh rate capability was further confirmed by galvanostatic charge and discharge profiles, showing symmetrical straight lines and no observable voltage drop at the beginning of the discharge curves for varying current densities (Figure 4b). Importantly, our UPSCs-25 exhibited excellent cycling stability without any capacitance loss after 50 000 cycles at 10 V s^{-1} (Figure 4c).

To evaluate the mechanical stability of such ultrathin devices for flexible energy storage, we further examined the

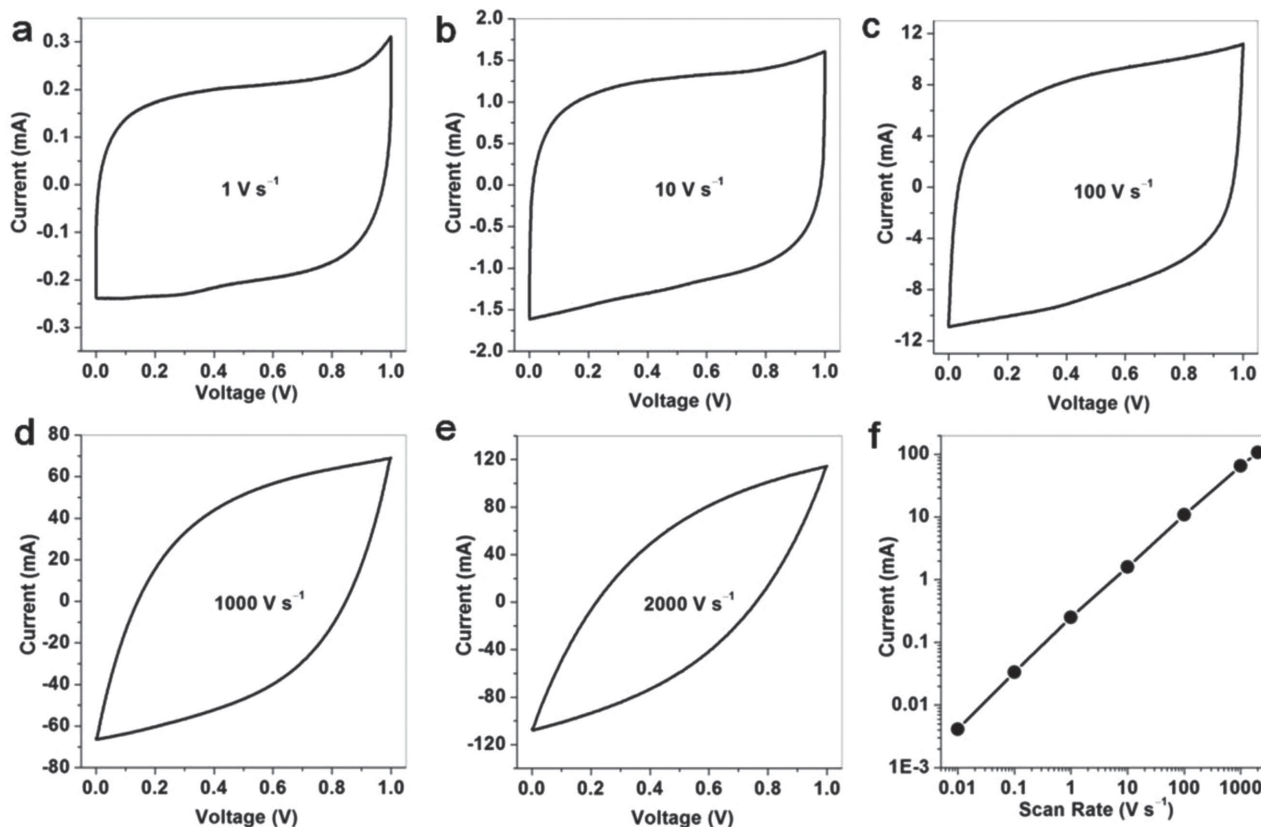


Figure 3. Electrochemical characterization of UPSCs-25. a–e) CV curves of UPSCs-25 obtained at different scan rates of: a) 1, b) 10, c) 100, d) 1000, and e) 2000 V s⁻¹. f) Plot of the discharge current as a function of the scan rate for UPSCs-25.

real performance of an as-fabricated device under constant bending conditions. In the normal bending state, e.g., flat, hung on a hair and put on a NMR glass tube (Figure 1i–l), the resulting UPSC devices exhibited stable performance without any capacitance fading, indicative of excellent mechanical flexibility. Moreover, under serious bending states of, e.g., 180° symmetrical folding and rolled up, the device measured at a high scan rate of 10 V s⁻¹ exhibited only a slight capacitance loss of <0.7% compared with the flat state, suggesting ultraflexibility and highly stable electrochemical performance (Figure 4d). This superior performance of our UPSCs under serious bending states cannot be realized using conventional, relatively rigid PET substrates (thickness of >200 μm).

The electrochemical performance of the UPSCs can be readily adjusted by varying the PH1000 ratio in the ink (Figure S4, Supporting Information) and the volume of ink (Figure S5, Supporting Information) used for the thin-film deposition. For instance, when the volume of spray-coated ink increased from 1 to 3 and 5 mL, the thickness of EG/PH1000 film increased from 25 to 77 and 128 nm, respectively (Figure S6, Supporting Information). The corresponding UPSCs based on the 77- and 128-nm-thick films were denoted as UPSCs-77 and UPSCs-128, respectively. When the thick film was used, the fabricated devices, e.g., UPSCs-77 and UPSCs-128, exhibited larger capacitive responses, as indicated by the CV measurements (Figure 5a). As a result, the areal capacitance

at 1 V s⁻¹ increased from 0.4 mF cm⁻² for UPSCs-25 to 1.2 mF cm⁻² for UPSCs-77 and 1.8 mF cm⁻² for UPSCs-128 upon increasing the film thickness, whereas the volumetric capacitance slightly decreased from 155 F cm⁻³ for UPSCs-25 to 153 F cm⁻³ for UPSCs-77 and 144 F cm⁻³ for UPSCs-128 (Figure 5b). Notably, these three resultant devices can still provide a significant areal capacitance of 0.15–0.5 mF cm⁻² and a volumetric capacitance of 38 to 62 F cm⁻³ even at a high scan rate, e.g., 100 V s⁻¹ (Figure S7, Supporting Information).

The electrochemical impedance spectra (EIS) of UPSCs-25, UPSCs-77, and UPSCs-128 are compared in Figure 5c,d. As observed in Figure 5c, the complex plane plots of UPSCs-25 showed a larger slope of closed 90° than UPSCs-77 and UPSCs-128 at a low frequency (Figure 5c), indicative of fast ion diffusion in these supercapacitors. Furthermore, a vertical line characteristic of capacitive behavior was also obtained in these plots, without the presence of the charge-transport semicircle of conventional supercapacitors at expanded high frequency (Figure 5d). A slight increase in the equivalent series resistance (ESR) was identified from 2.28 to 2.39 and 2.56 Ω for UPSCs-25, UPSCs-77, and UPSCs-128, respectively, which was attributed to an elongation of the ionic diffusion paths in the thickened films with polymer gel electrolyte.

Figure 5e displays the dependence of the phase angle on the frequency of UPSCs-25, UPSCs-77, and UPSCs-128. The transition between the resistor and capacitor becomes smooth

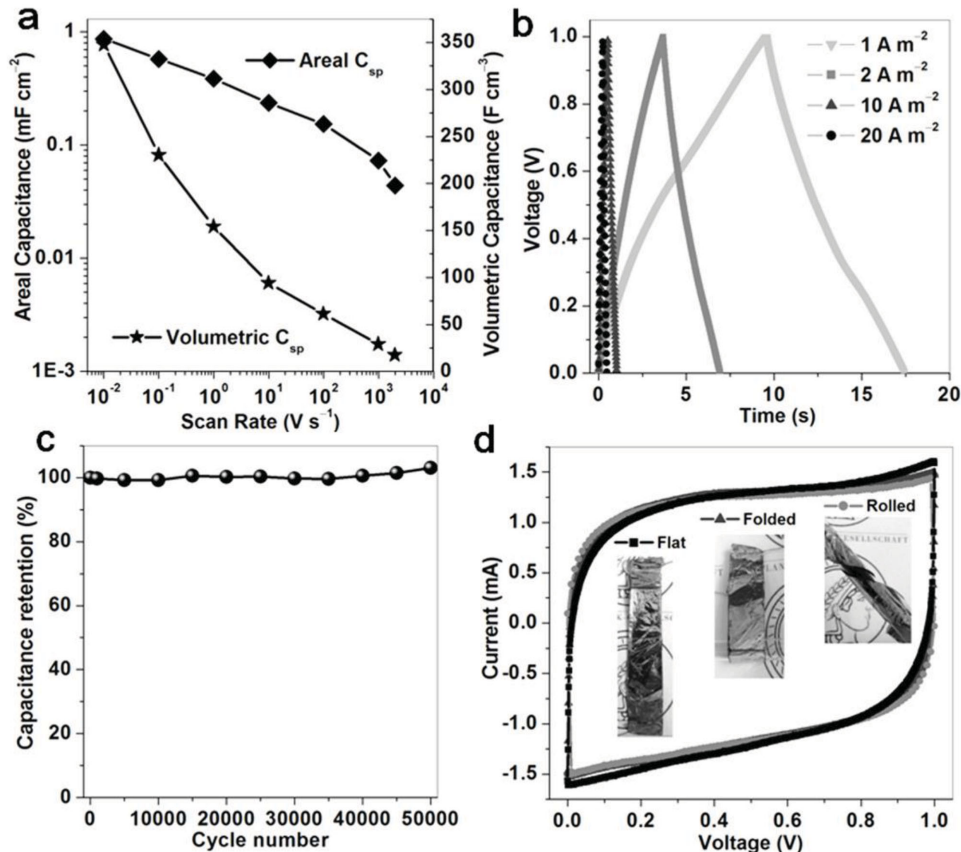


Figure 4. Evolution of specific capacitance and cycling stability of UPSCs-25. a) Areal capacitance and volumetric capacitance of UPSCs-25. b) Galvanostatic charge and discharge curves of UPSCs-25 at varying current densities of 1, 2, 10, and 20 A m⁻². c) Cyclic stability of UPSCs-25. d) CV curves determined for UPSCs-25 under three different bending states. Inset: digital images of three different bending states: flat, folded, and rolled.

(Figure 5e), similar to electrolytic capacitors,^[21] which is mainly attributable to the superior ion-transport of graphene over porous carbon.^[21] Moreover, the characteristic frequency f_0 at the phase angle of -45° decreases with increasing film thickness, 1000 Hz for UPSCs-25, 708 Hz for UPSCs-77, and 320 Hz for UPSCs-128 (Figure 5e and Figure S8, Supporting Information). Nevertheless, the relaxation time constant τ_0 ($\tau_0 = 1/f_0$, the device needs the minimum time for discharging its maximum energy of $\geq 50\%$) only increased, for instance, 1.0 ms for UPSCs-25, 1.5 ms for UPSCs-77, and 2.9 ms for UPSCs-128 (Figure S8, Supporting Information), which is indicative of ultrahigh fast ion diffusion in our devices. Notably, the relaxation time constant τ_0 of UPSCs-25 of 1 ms is three orders of magnitude lower than that of the typical active carbon-based EDLCs (ca. 1 s),^[21] much shorter than those of high-rate EDLCs based on onion-like carbon (26 ms)^[35] and graphene film (13.3 ms),^[43] and comparable to those of the state-of-the-art ultrahigh-power supercapacitors with vertically oriented graphene (0.067 ms)^[21] and ErGO (0.17–1 ms).^[22]

Considering the vertical line characteristic of the Nyquist plot at low frequencies and short relaxation time constant, we further utilized a series-RC circuit model to assess the RC time constant in terms of the equation $\tau_{RC} = C \times Z'$, where Z' is the resistance

derived from the real part of the impedance (Ω), and C is the device capacitance calculated from the equation $C = -1/(2\pi fZ'')$, where f is the frequency (Hz) and Z'' is the imaginary part of the impedance (Ω).^[21,22] The resulting plot of the capacitance versus frequency for UPSCs-25, UPSCs-77, and UPSCs-128 is presented in Figure 5f. Notably, at 120 Hz, the UPSCs-25, UPSCs-77, and UPSCs-128 exhibited a derived capacitance value of 75, 127, and 179 μF , respectively, and a measured resistance of 6.3, 4.7, and 3.6 Ω , respectively. Thus, a RC time constant of 472, 597, and 644 μs was achieved for UPSCs-25, UPSCs-77, and UPSCs-128, respectively. These values are well comparable to those of the state-of-the-art EDLCs based on vertically oriented graphene (<200 μs),^[21] ErGO (1.35 ms),^[22] and thermally reduced GO (2.3 ms).^[23] This result suggests that our printable supercapacitors hold great potential to replace AECs (that need 8.3 ms) for AC line-filtering applications.^[21,22] Additionally, the Ragone plot revealed that the energy density and power density (based on two electrodes) were 12 mW h cm⁻³ and 4386 W cm⁻³ for our UPSCs (Figure S9, Supporting Information), respectively, which could potentially fill the gap between high-energy lithium thin-film batteries (10 mW h cm⁻³)^[35] and high-power electrolytic capacitors (10³ W cm⁻³).^[41]

In summary, we have demonstrated a simple but scalable manufacturing technique that could potentially be adopted

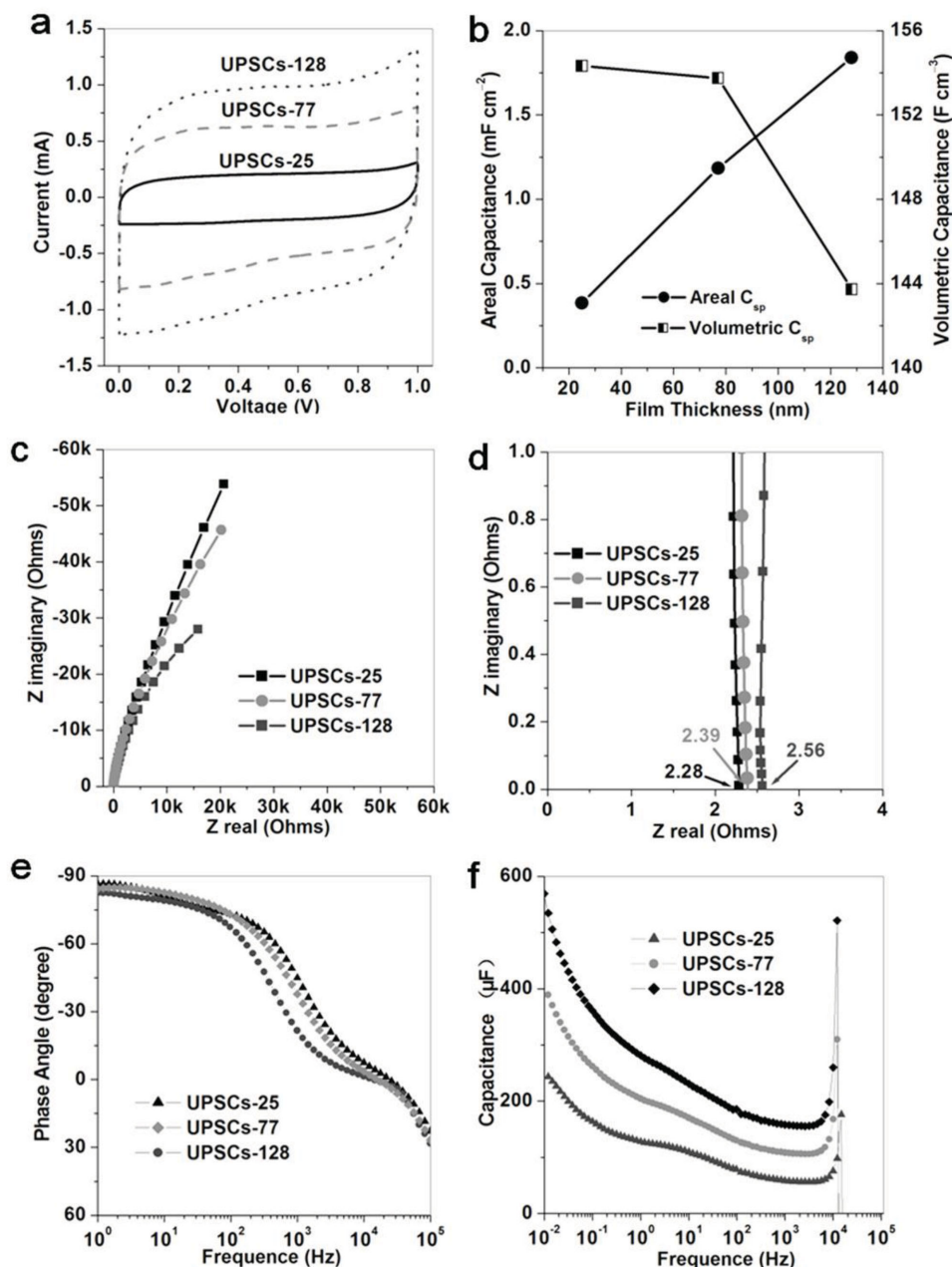


Figure 5. Comparison of UPSCs-25, UPSCs-77 and UPSCs-128. a) CV curves and b) areal capacitance and volumetric capacitance of UPSCs-25, UPSCs-77, and UPSCs-128 measured at 1 V s⁻¹. c) Complex plane plot of the impedance and d) magnified plot of the high-frequency region (c) of UPSCs-25, UPSCs-77, and UPSCs-128. e) Impedance phase angle as a function of frequency, and f) plot of capacitance versus frequency of UPSCs-25, UPSCs-77, and UPSCs-128.

for large-scale production of UPSCs using spray coating of solution-processed high-quality EG/PH1000 films on ultrathin PET substrates. The technique proposed here is a fast, convenient, and efficient strategy for producing these printable supercapacitors, which possessed an unprecedented volumetric capacitance of 348 F cm⁻³, an ultrahigh rate of up to 2000 V s⁻¹, and excellent cycling stability (without any capacitance loss after 50 000 cycles). Furthermore, our device exhibited excellent flexibility under an arbitrary bending state and an AC line-filtering performance with a low RC time constant of <1 ms,

outperforming commercially available AECs. Therefore, these UPSCs with AC line-filtering performance are promising for powering various printed electronics with thin, lightweight, portable, and wearable features for high energy density, power density, and frequency operation.

Supporting Information

Supporting Information is available from the Wiley Online Library or from the author.

Acknowledgements

This work was financially supported by the ERC Grant through 2DMATER and NANOGRAPH, DFG SPP 1459, and EC under Graphene Flagship (Grant No. CNECT-ICT-604391).

Received: March 12, 2015

Revised: April 13, 2015

Published online:

- [1] J. H. Ahn, H. S. Kim, K. J. Lee, S. Jeon, S. J. Kang, Y. G. Sun, R. G. Nuzzo, J. A. Rogers, *Science* **2006**, 314, 1754.
- [2] D. Hecht, *Mater. Today* **2009**, 12, 10.
- [3] J. S. Shi, C. X. Guo, M. B. Chan-Park, C. M. Li, *Adv. Mater.* **2012**, 24, 358.
- [4] S. H. Kim, K. Hong, W. Xie, K. H. Lee, S. P. Zhang, T. P. Lodge, C. D. Frisbie, *Adv. Mater.* **2013**, 25, 1822.
- [5] M. Kaltenbrunner, M. S. White, E. D. Glowacki, T. Sekitani, T. Someya, N. S. Sariciftci, S. Bauer, *Nat. Commun.* **2012**, 3, 770.
- [6] Z. S. Wu, X. L. Feng, H. M. Cheng, *Natl. Sci. Rev.* **2014**, 1, 277.
- [7] M. Kaempgen, C. K. Chan, J. Ma, Y. Cui, G. Gruner, *Nano Lett.* **2009**, 9, 1872.
- [8] T. Chen, Y. H. Xue, A. K. Roy, L. M. Dai, *ACS Nano* **2014**, 8, 1039.
- [9] H. Y. Jung, M. B. Karimi, M. G. Hahm, P. M. Ajayan, Y. J. Jung, *Sci. Rep.* **2012**, 2, 3612.
- [10] B. G. Choi, J. Hong, W. H. Hong, P. T. Hammond, H. Park, *ACS Nano* **2011**, 5, 7205.
- [11] X. H. Lu, G. M. Wang, T. Zhai, M. H. Yu, S. L. Xie, Y. C. Ling, C. L. Liang, Y. X. Tong, Y. Li, *Nano Lett.* **2012**, 12, 5376.
- [12] Z. Weng, Y. Su, D. W. Wang, F. Li, J. H. Du, H. M. Cheng, *Adv. Energy Mater.* **2011**, 1, 917.
- [13] J. Keskinen, E. Sivonen, S. Jussila, M. Bergelin, M. Johansson, A. Vaari, M. Smolander, *Electrochim. Acta* **2012**, 85, 302.
- [14] S. Lehtimäki, M. Li, J. Salomaa, J. Pöyhönen, A. Kalanti, S. Tuukkanen, P. Heljo, K. Halonen, D. Lupo, *Int. J. Electr. Power Energy Syst.* **2014**, 58, 42.
- [15] X. B. Ji, P. M. Hallam, S. M. Houssein, R. Kadara, L. M. Lang, C. E. Banks, *RSC Adv.* **2012**, 2, 1508.
- [16] C. Pochiang, C. Haitian, Q. Jing, Z. Chongwu, *Nano Res.* **2010**, 3, 594.
- [17] Y. F. Xu, M. G. Schwab, A. J. Strudwick, J. Hennig, X. L. Feng, Z. S. Wu, K. Müllen, *Adv. Energy Mater.* **2013**, 3, 1035.
- [18] X. Zhao, C. Johnston, A. Crossley, P. S. Grant, *J. Mater. Chem.* **2010**, 20, 7637.
- [19] Y. F. Xu, I. Hennig, D. Freyberg, A. J. Strudwick, M. G. Schwab, T. Weitz, K. C. P. Cha, *J. Power Sources* **2014**, 248, 483.
- [20] J. Yeo, G. Kim, S. Hong, M. S. Kim, D. Kim, J. Lee, H. B. Lee, J. Kwon, Y. D. Suh, H. W. Kang, H. J. Sung, J. H. Choi, W. H. Hong, J. M. Ko, S. H. Lee, S. H. Choa, S. H. Ko, *J. Power Sources* **2014**, 246, 562.
- [21] J. R. Miller, R. A. Outlaw, B. C. Holloway, *Science* **2010**, 329, 1637.
- [22] K. X. Sheng, Y. Q. Sun, C. Li, W. J. Yuan, G. Q. Shi, *Sci. Rep.* **2012**, 2, 247.
- [23] T. Nathan-Walleiser, I. M. Lazar, M. Fabritius, F. J. Tolle, Q. Xia, B. Bruchmann, S. S. Venkataraman, M. G. Schwab, R. Mulhaupt, *Adv. Funct. Mater.* **2014**, 24, 4706.
- [24] X. Y. Lang, A. Hirata, T. Fujita, M. W. Chen, *Nat. Nanotechnol.* **2011**, 6, 232.
- [25] Z. Bo, W. G. Zhu, W. Ma, Z. H. Wen, X. R. Shuai, J. H. Chen, J. H. Yan, Z. H. Wang, K. F. Cen, X. L. Feng, *Adv. Mater.* **2013**, 25, 5799.
- [26] K. Parvez, Z.-S. Wu, R. Li, X. Liu, R. Graf, X. Feng, K. Müllen, *J. Am. Chem. Soc.* **2014**, 136, 6083.
- [27] K. Parvez, R. J. Li, S. R. Puniredd, Y. Hernandez, F. Hinkel, S. H. Wang, X. L. Feng, K. Müllen, *ACS Nano* **2013**, 7, 3598.
- [28] Z. Liu, K. Parvez, R. Li, R. Dong, X. Feng, K. Müllen, *Adv. Mater.* **2014**, 27, 669.
- [29] Z. S. Wu, A. Winter, L. Chen, Y. Sun, A. Turchanin, X. Feng, K. Müllen, *Adv. Mater.* **2012**, 24, 5130.
- [30] Z. S. Wu, K. Parvez, A. Winter, H. Vieker, X. Liu, S. Han, A. Turchanin, X. Feng, K. Müllen, *Adv. Mater.* **2014**, 26, 4552.
- [31] Z. S. Wu, Y. Sun, Y. Z. Tan, S. B. Yang, X. L. Feng, K. Müllen, *J. Am. Chem. Soc.* **2012**, 134, 19532.
- [32] U. N. Maiti, J. Lim, K. E. Lee, W. J. Lee, S. O. Kim, *Adv. Mater.* **2014**, 26, 615.
- [33] Z. S. Wu, K. Parvez, X. L. Feng, K. Müllen, *Nat. Commun.* **2013**, 4, 2487.
- [34] Z. S. Wu, K. Parvez, X. Feng, K. Müllen, *J. Mater. Chem. A* **2014**, 2, 8288.
- [35] D. Pech, M. Brunet, H. Durou, P. H. Huang, V. Mochalin, Y. Gogotsi, P. L. Taberna, P. Simon, *Nat. Nanotechnol.* **2010**, 5, 651.
- [36] W. Gao, N. Singh, L. Song, Z. Liu, A. L. M. Reddy, L. J. Ci, R. Vajtai, Q. Zhang, B. Q. Wei, P. M. Ajayan, *Nat. Nanotechnol.* **2011**, 6, 496.
- [37] X. W. Yang, C. Cheng, Y. F. Wang, L. Qiu, D. Li, *Science* **2013**, 341, 534.
- [38] Y. X. Xu, Z. Y. Lin, X. Zhong, X. Q. Huang, N. O. Weiss, Y. Huang, X. F. Duan, *Nat. Commun.* **2014**, 5, 4554.
- [39] M. Ghaffari, Y. Zhou, H. Xu, M. Lin, T. Y. Kim, R. S. Ruoff, Q. M. Zhang, *Adv. Mater.* **2013**, 25, 4879.
- [40] Y. W. Zhu, S. Murali, M. D. Stoller, K. J. Ganesh, W. W. Cai, P. J. Ferreira, A. Pirkle, R. M. Wallace, K. A. Cychosz, M. Thommes, D. Su, E. A. Stach, R. S. Ruoff, *Science* **2011**, 332, 1537.
- [41] M. F. El-Kady, V. Strong, S. Dubin, R. B. Kaner, *Science* **2012**, 335, 1326.
- [42] M. F. El-Kady, R. B. Kaner, *Nat. Commun.* **2013**, 4, 1475.
- [43] X. W. Yang, J. W. Zhu, L. Qiu, D. Li, *Adv. Mater.* **2011**, 23, 2833.